Available online at www.sciencedirect.com
ScienceDirect
Catalysis Today 120 (2007) 126–132
CATALYSIS TODAY
www.elsevier.com/locate/cattod

Effect of alkali-ion-doping on the local structure and the photocatalytic properties of alumina-supported vanadium oxides

Fumiaki Amano, Tsuyoshi Yamaguchi, Tsunehiro Tanaka *

Department of Molecular Engineering, Graduate School of Engineering, Kyoto University, Kyoto 615-8510, Japan

Available online 1 September 2006

Abstract

The influence of alkali-ion-doping on supported vanadium oxide was investigated for selective photocatalytic oxidation of propylene with molecular oxygen. V_2O_5/Al_2O_3 shows higher selectivity to propenal formation than V_2O_5/SiO_2. Alkali-ion-doping resulted in a significant enhancement of the photocatalytic capability for the propenal formation. Among alkali ions of Li, Na, K, and Rb, rubidium ion was found to be the most effective modifier. The Rb-ion-modified V_2O_5/Al_2O_3 was characterized by means of XAFS, FT-IR, Raman, and UV–vis diffuse reflectance spectroscopies. The terminal V=O bond of monomeric VO_4 tetrahedron was elongated by an interaction with a Rb ion. The photocatalytic active site was found to be the Rb-ion-modified VO_4 monomer bound to alumina surface through three V–O bonds. In contrast, metavanadate chains were not effective for the photocatalytic reaction.

Keywords: Alkali-ion-doping; Oxidative dehydrogenation (ODH); Vanadium

1. Introduction

Supported vanadium oxide catalyzes oxidative dehydrogenation (ODH) of light alkanes with superior activity and selectivity [1–5]. The acid–base characters and the redox properties are two of the important factors in the ODH reactions [1,2]. Doping of alkali ions, in particular potassium ion, on supported vanadium oxides is known to increase the selectivity to corresponding alkenes formation, although the catalytic activity was decreased due to the retarding of the redox property [3–5]. The presence of alkali ions resulted in a decrease of the number of acid sites on which a formation of carbon oxides and an isomerization of alkenes are promoted. The most striking role of alkali ion is considered to be the basic properties suppressing the surface acidity [4–6].

The effect of alkali addition on the surface structure has also been investigated in supported vanadium oxides [5–11]. With the studies of Raman [5–9], FT-IR [10], and EXAFS [8] spectroscopies, the elongation of the terminal V=O bond of the isolated VO_4 tetrahedron was found in alkali-ion-doped supported vanadium oxides. In the case of the isolated VO_4 tetrahedron on silica, an alkali addition weakened the vibrational fine structures in the phosphorescence emission [11], which is generally attributed to the terminal V=O bond stretching [12,13]. These results prove the structural change of the isolated VO_4 tetrahedron and the interaction between alkali ions and the terminal V=O bonds. From the results of EXAFS analysis and ab initio molecular orbital calculation, a model K–VO_4 cluster, two bonds of which are interacted with an alkali ion, has been proposed on K-ion-doped silica-supported vanadium oxide (V_2O_5/SiO_2) [8].

The isolated VO_4 species on silica, $(SiO)_3V{=}O$, promote photocatalytic partial oxidation of light alkanes and alkenes with molecular oxygen under UV irradiation [14–17]. The electron transition to the anti-bonding orbital of the terminal V=O bond ($n \rightarrow \pi^*$ transition) destabilizes and activates the lattice oxygen [17,18]. The isolated VO_4 species in the photo-excited triplet state is assumed to be active for photocatalytic oxidation. It is found that the alkali-ion-doped V_2O_5/SiO_2 exhibit higher photocatalytic activity, selectivity, and stability than the non-modified catalysts for the photocatalytic oxidation [11,19–22]. The modification of the local environment and the electronic state by alkali ion would be responsible for the high photocatalytic activity and the products selectivity.

* Corresponding author. Tel.: +81 75 383 2558; fax: +81 75 383 2561.
E-mail address: tanakat@moleng.kyoto-u.ac.jp (T. Tanaka).

0920-5861/$ – see front matter
doi:10.1016/j.cattod.2006.07.041

Recently, alumina-supported vanadium oxides (V_2O_5/Al_2O_3) are found to be effective photocatalysts for liquid-phase oxidation of cyclohexane under UV irradiation without considerable leaching of the vanadium species from solid to the solution [23–25]. There are a few reports about the photocatalysis over alumina-supported ones. The effect of alkali doping on the surface vanadium oxides on alumina has not been investigated. If there is a direct interaction between the photocatalytic vanadium center and the alkali ion, the doping effect will be observed irrespective of the kinds of support materials. Therefore, we investigated the effect of alkali-ion-doping on V_2O_5/Al_2O_3 for selective photocatalytic oxidation using molecular oxygen.

2. Experimental

2.1. Materials

Amorphous silica was prepared by the hydrolysis of tetraethyl orthosilicate (TEOS) in a water–ethanol mixture at the boiling points, followed by calcination in dry air at 773 K for 5 h. γ-Alumina (JRC-ALO-8) was provided by the Catalysis Society of Japan. The supported vanadium oxide catalysts were prepared by impregnation of the silica or alumina (3.0 g) with an aqueous solution (100 ml) dissolving the necessary amount of NH_4VO_3 at 353 K for 2 h, followed by evaporation to dryness. Li, Na, K, and Rb-ion-modified catalysts were also prepared by impregnation of the silica or alumina with an aqueous solution of NH_4VO_3 and each alkali hydroxide (LiOH, NaOH, KOH, and RbOH). After the evaporation, the samples were dried at 373 K for overnight and subsequently calcined in dry air at 773 K for 5 h. The V_2O_5/SiO_2 and the alkali-ion-modified V_2O_5/SiO_2 were labeled *x*VS and alkali-*x*VS, respectively. The V_2O_5/Al_2O_3 and the alkali-ion-modified V_2O_5/Al_2O_3 were labeled *x*VA and alkali-*x*VA, respectively. The *x* denotes the V_2O_5 wt% in the samples. The molar ratio of alkali ions to vanadium ions (alkali/V) was typically adjusted to 1.5 and varied in the region of 0.5–5. The BET specific surface area was measured by nitrogen adsorption at 77 K using BELSORP 28SA.

2.2. Spectroscopies

Prior to the measurements at dehydrated condition, the samples were evacuated for 1 h and calcined with 80 Torr of oxygen for 2 h at 673 K, followed by evacuation at the same temperature. The spectra of the dehydrated sample were recorded without exposure to the open air. The UV–vis diffuse reflectance spectra were recorded using a Perkin-Elmer Lambda-19 spectrometer equipped with an integrating sphere. $BaSO_4$ was used as a standard reflection sample. V-K edge X-ray absorption experiments were carried out on the BL-9A at Photon Factory of the High Energy Accelerator Research Organization (Tsukuba, Japan) and recorded in a fluorescence mode with a Si(1 1 1) two-crystal monochromator. The data reduction method of XAFS (XANES and EXAFS) spectra has been previously reported in detail [26]. The photon energy was calibrated by the pre-edge peak position in the absorption spectrum of V_2O_5 crystallite (5470 eV). The Fourier transforms of k^3-weighted EXAFS spectra were obtained in the *k* range of 3.5–11.5 $Å^{-1}$.

FT-IR spectra were obtained using a Perkin-Elmer Spectrum One in a transmission mode at room temperature. The 10 mg of sample was pressed into a self-supporting wafer and mounted in an in situ cell equipped with BaF_2 windows. The wafer was pretreated at 673 K and measured at dehydrated state. The data acquisitions consisted of 10 spectra with a resolution of 4 cm^{-1}.

Laser Raman and powder X-ray diffraction (XRD) patterns were recorded under ambient conditions at room temperature. The laser Raman spectra were obtained with the 514.5 nm line of an $argon^+$ laser emission and an incident laser power of 100 mW and a resolution of 14.5 cm^{-1} using a JASCO NRS-2000. The data acquisition consisted from 16 spectra with scan times of 3–60 s depending on the signal level. The XRD patterns were obtained using Shimadzu XD-D1 with Cu Kα radiation (averaged as 1.5418 Å).

2.3. Photoreaction test

Photooxidation of propylene was carried out under a gas mixture of 20% C_3H_6/10% O_2/70% He at a total flow rate of

Table 1
Results of photocatalytic oxidation of propylene with molecular oxygen at 373 K

Sample	V_2O_5 loading (wt%)	Rb_2O loading (wt%)	A_{BET}[a] ($m^2\ g^{-1}$)	C_3H_6 conversion rate (μmol h^{-1})	Selectivity (%)				Acrolein formation rate (μmol h^{-1})
					Propenal	C_3[b]	Ethanal	CO_2	
0.1VS	0.1	0.0	590	52	15	42 (38)[c]	32	11	8
2.5VS	2.5	0.0	588	30	17	25 (14)[c]	46	12	5
Rb-2.5VS	2.5	3.8[d]	179	244	36	6	7	51	88
Al_2O_3	0.0	0.0	154	7	n.d.	13	6	81	n.d.
2.5VA	2.5	0.0	152	29	41	6	23	30	12
Rb-2.5VA	2.5	3.8[d]	154	67	56	5	8	31	38
Rb_2O/Al_2O_3	0.0	2.5	152	15	11	14	12	63	2
$RbVO_3$	49.3	50.7	–	3	92	8	n.d.	n.d.	3

The data were obtained at 300 min on stream.
[a] BET specific surface area.
[b] The C_3 oxygenated products except propenal: propanal, propylene oxide, and acetone.
[c] The selectivity to propylene oxide are shown in the parenthesis.
[d] The molar ratio of rubidium to vanadium (Rb/V) was adjusted to 1.5.

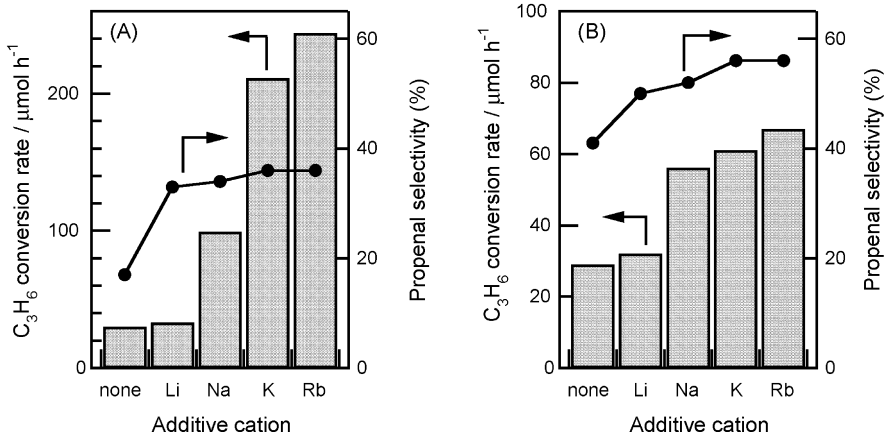

Fig. 1. The effect of alkali ion addition on: 2.5VS (A) and 2.5VA (B) in the photocatalytic oxidation of propylene. The molar ratio of alkali to vanadium (alkali/V) was adjusted to 1.5.

100 ml min^{-1} at an atmospheric pressure. About 350 mg of catalyst (particulate size 26–50 mesh) was packed in a flow cell (volume 0.75 ml, irradiated area 7.5 cm^2) made of quartz glass and heated at 673 K under He balanced 20% O_2 stream at flow rate of 50 ml min^{-1} for 2 h prior to a reaction. The light was irradiated from a 300 W xenon arc lamp (Perkin-Elmer, CERAMAX PE300BUV) with reflection by a cold mirror that can permit UV–vis light with $240 < \lambda < 440$ nm. The temperature of the catalyst bed was adjusted to 373 K during the irradiation by a mantle heater. The products were analyzed by gas chromatographs (a PEG 20M column with an flame ionization detector and a Shincarbon T column with a thermal conductivity detector) connected directly to a flow reactor.

3. Results and discussion

3.1. Effect of alkali-ion-doping on supported V_2O_5 catalyst

Table 1 summarizes the results of photooxidation of propylene with molecular oxygen under UV irradiation at 373 K, in which the photo-generated products were propenal, propylene oxide, acetone, propanal, ethanal, and carbon dioxide. The distribution of the photo-generated products significantly depends on the vanadium loading of VS. Low loaded VS (0.1 wt%) exhibits high selectivity to propylene oxide formation [17]. In contrast, 2.5VS shows non-selective oxidation to various C_3 oxygenated products. As previously reported, an alkali ion addition to VS drastically enhanced the photocatalytic activity and the selectivity to propenal formation. Fig. 1A shows the effect of additive cation on 2.5VS for the photocatalytic oxidation of propylene. Li, Na, K, and Rb ions gave the similar effect upon the selectivity to propenal. Among these alkali ions, Rb ion was found to be the most suitable modifier. The photocatalytic activity of Rb-ion-modified 2.5VS is eight times higher than that of non-modified 2.5VS, although the specific surface area is small due to the high pH value in the solution using for catalyst preparation.

VA shows high selectivity to propenal formation in contrast to VS. This indicates that the nature of alumina surface influenced the photocatalytic properties. The addition of alkali ions also improves the photocatalytic capability for propenal formation over VA. Fig. 1B shows the effect of additive cation on the 2.5VA. The photocatalytic activity was gradually increased in the order of Na < K < Rb. The propenal yield of Rb-ion-modified 2.5VA is three times higher than that of non-modified 2.5VA. Because bare alumina and Rb_2O/Al_2O_3 are not effective for propenal formation, the interaction between the surface vanadium oxides and the alkali ion is important for the increase of photocatalytic activity. In the case of alumina support, the specific surface area was not decreased by addition of RbOH to the solution for catalyst preparation.

3.2. Effect of vanadium loading on Rb-ion-modified V_2O_5/Al_2O_3

Fig. 2A shows the dependence of the V_2O_5 loading on the products yield over Rb-VA. The Rb/V molar ratio was adjusted to 1.5. The propenal yield was monotonically increased with an increase of V_2O_5 loading until 3.5 wt%. This means that the number of photocatalytic active site for propenal formation was saturated around 3.5 wt% and a photo-inactive vanadium species was formed at higher loading.

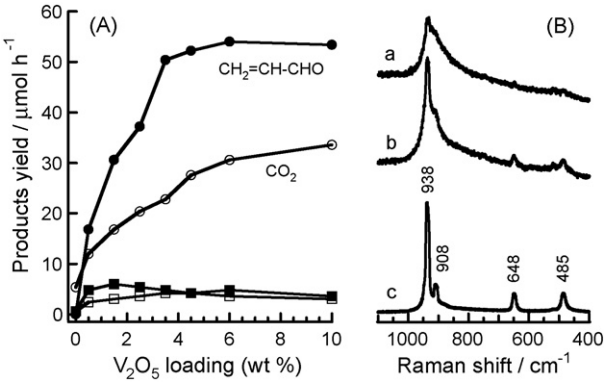

Fig. 2. (A) The effect of V_2O_5 loading on the photocatalytic oxidation of propylene over Rb-VA (Rb/V ratio = 1.5); propenal (●), carbon dioxide (○), ethanal (■), and the other C_3 oxygenated products (□). (B) Raman spectra of: (a) Rb-2.5VA, (b) Rb-3.5VA, and (c) Rb-6.0VA.

Fig. 2B shows Raman spectra of Rb-VA with various vanadium loadings. The Raman bands corresponding to rubidium metavanadate ($RbVO_3$; 938, 908, 648, and 485 cm^{-1}) were clearly observed in Rb-6.0VA. There was no XRD pattern due to $RbVO_3$ crystallite in Rb-6.0VA. Therefore, the crystal size of the metavanadate chains is very small. The formation of amorphous KVO_3 clusters has been reported in K-ion-doped V_2O_5/TiO_2 [9,27]. The molecular structure of sodium metavanadate, $NaVO_3$, consists of corner-sharing tetrahedral VO_4 chains with two V–O distances, so-called metavanadate chains [28], and the Raman spectra of NH_4VO_3, $NaVO_3$, KVO_3, and $RbVO_3$ were almost same. It is noted that even in the case of Rb-3.5VA catalyst, a trace of peaks due to metavanadate chains was detected. However, the fraction of the chains to the total vanadium species in the sample would be very low, since the crystallites like $RbVO_3$ generally give much stronger Raman signals than the surface metal oxide species (typically by a factor of 10^1–10^2) [6,29].

3.3. Effect of Rb ion content on Rb-ion-modified V_2O_5/Al_2O_3

Fig. 3A shows the dependence of the Rb/V molar ratio on the product yield over Rb-3.5VA. The propenal production was monotonically increased with an increase of Rb/V value until 1.5 and maximized when the Rb/V molar ratio is around 1.5. The sample with high Rb content (Rb/V = 5.0) exhibits low propenal yield. Since the relatively high amount of alkali ion is necessary for the modification of catalyst, the improvement of the photocatalytic activity and selectivity would not be derived from the suppression of surface acidity but the structural change of vanadium species by alkali ion. It has been reported that the surface structure of the vanadium oxides are depending on both the V_2O_5 loading and the alkali ion content [9,27].

Fig. 3B shows Raman spectra of Rb-3.5VA with different Rb/V molar ratios. In the case of non-modified 3.5VA, the surface vanadium density was 1.5V-atom nm^{-2}, which corresponds to 0.16 monolayer (1.0 monolayer calculated for bulk V_2O_5 = 9.5V-atom nm^{-2}) [30]. There was no Raman band due to V_2O_5 crystallite. In the present low surface density, the

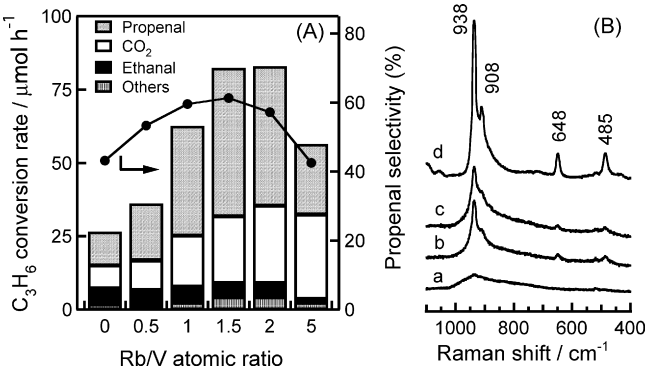

Fig. 3. (A) The effect of Rb/V molar ratio on the photocatalytic oxidation of propylene over Rb-3.5VA catalysts; products: propenal, carbon dioxide, ethanal, and the other C_3 oxygenated products (propylene oxide, propanal, and acetone). (B) Raman spectra of Rb-3.5VA: (a) Rb/V = 0.5, (b) Rb/V = 1.5, (c) Rb/V = 2, and (d) Rb/V = 5.

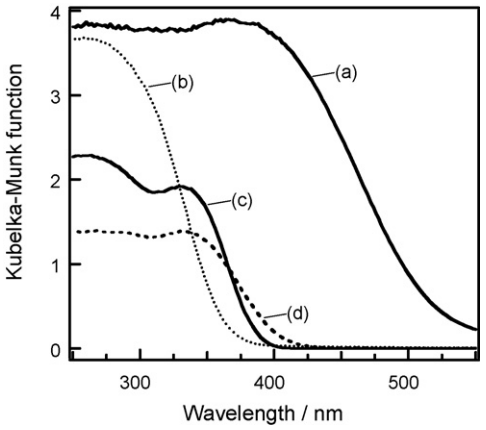

Fig. 4. UV–vis diffuse reflectance spectra of silica-based catalysts: (a) hydrated 2.5VS, (b) dehydrated 2.5VS, (c) hydrated Rb-2.5VS, and (d) dehydrated Rb-2.5VS.

surface vanadium oxides are present on alumina surface in a highly dispersed state like tetrahedral VO_4 monomer [31]. In contrast, the presence of metavanadate chains (938, 908, 648, and 485 cm^{-1}) was clearly confirmed at Rb-3.5VA with Rb/V value of 5.0. In the case of Rb/V value of 1.5–2.0, metavanadate chains are very minor species since the Raman bands are ambiguous. Therefore, the low yield of propenal at high Rb/V ratio is derived from the generation of considerable amount of metavanadate chains. It is suggested that the photocatalytic active site is the Rb-ion-modified vanadium species in a highly dispersed state rather than the oligomeric metavanadate chains.

Supported vanadium oxides show ligand to metal charge transfer (LMCT) bands from O^{2-} to V^{5+} in the 200–500 nm region. Fig. 4 shows diffuse reflectance spectra of silica-based catalysts at hydrated and dehydrated state. It is well known that the surface structure of V_2O_5/SiO_2 is significantly affected by water adsorption. At hydrated state, the spectrum of 2.5VS resembles to that of bulk V_2O_5, indicating the presence of VO_5/VO_6 polymers on silica. When the 2.5VS was dehydrated, the LMCT band was shifted to lower wavelength due to the dispersion of the VO_5/VO_6 polymers. From the absorption edge energy, the vanadium species in dehydrated 2.5VS is revealed

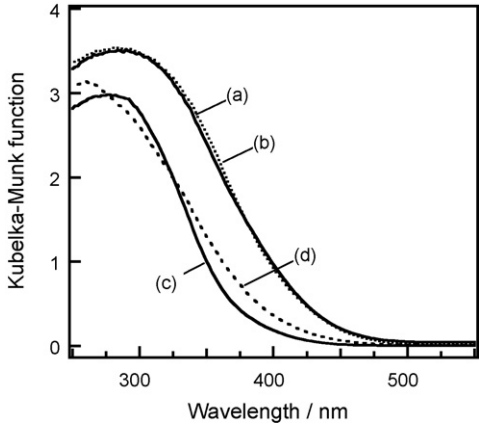

Fig. 5. UV–vis diffuse reflectance spectra of silica-based catalysts: (a) hydrated 2.5VA, (b) dehydrated 2.5VA, (c) hydrated Rb-2.5VA, and (d) dehydrated Rb-2.5VA.

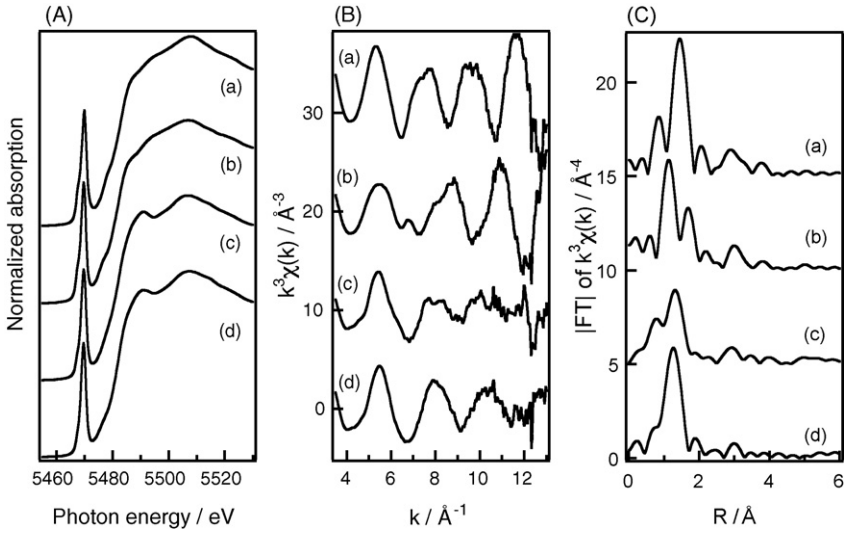

Fig. 6. V-K edge XANES spectra (A), EXAFS spectra (B), and Fourier transforms of the EXAFS spectra (C) of: 2.5VS (a), Rb-2.5VS (b), 2.5VA (c), and Rb-2.5VA (d) at dehydrated state. Fourier transforms was performed on EXAFS in the 3.5–11.5 $Å^{-1}$.

to be an isolated VO_4 tetrahedron [17]. In the case of Rb-2.5VS, the absorption band is significantly different from that of 2.5VS. The addition of Rb ion prevents the formation of the VO_5/VO_6 polymers in the presence of water molecule. There are two peaks in the LMCT absorption band in Rb-2.5VS, indicating the presence of two kinds of oxygen ligand.

Fig. 5 shows diffuse reflectance spectra of alumina-based catalysts at hydrated and dehydrated state. There is no effect of water molecules on the surface structure of vanadium species in 2.5VA. This would be due to a strong binding of the highly dispersed VO_4 tetrahedron by alumina surface. In the case of Rb-2.5VA, the spectra show a little difference between the hydrated and dehydrated state. The addition of Rb ion to 2.5VA causes the shift of the LMCT band to lower wavelength. In general, the blue shift of LMCT band of surface vanadium oxide suggests the decrease of the coordination number and/or the degree of polymerization [31]. However, we think that the present blue shift is because of the variance of the property of the oxygen ligand of tetrahedral VO_4 monomer on alumina. In order to elucidate this point, we investigated the local environment of the alkali-ion-modified vanadium species by means of XAFS spectroscopy.

Fig. 6A shows V-K edge XANES spectra of dehydrated samples with 2.5 wt% of V_2O_5 loading. All the XANES spectra have a sharp pre-edge peak around 5470 eV. The peak is attributed to 1s–3d dipole transitions allowed by destruction of the inversion symmetry around V atom [26,32]. From the pre-edge peak intensity, it is suggested that the vanadium oxide species are in tetrahedral symmetry. As previously reported, the presence of Rb ion did not change the tetrahedral structure of a surface vanadium species greatly [8]. Noted that the post-edge features are strongly dependent on the kinds of support.

Table 2
Results of curve fitting analysis for V–O shells of supported vanadium oxides

Sample	CN[a]	R[b] (Å)	$\Delta\sigma^{2}$[c] ($Å^2$)	R-factor[d] (%)
2.5VS	1.0	1.62	−0.0038	11.8
	3.0	1.81	−0.0025	
Rb-2.5VS	2.0	1.65	−0.0022	12.8
	2.0	1.87	0.0008	
2.5VA	1.0	1.56	0.0011	12.1
	2.9	1.72	0.0027	
Rb-2.5VA	0.8	1.69	−0.0012	5.5
	2.8	1.71	0.0091	

Inverse Fourier range, $\Delta R = 0.9$–1.9 $Å^{-1}$; fitting range, $\Delta k = 4.5$–10.5 $Å^{-1}$.
[a] Coordination number.
[b] Interatomic distance.
[c] Relative Debye–Waller factor against that of reference compound Na_3VO_4.
[d] $\sqrt{\sum_k [\chi_{obs}(k) - \chi_{calc}(k)]^2 / \sum_k \chi_{obs}(k)^2}$.

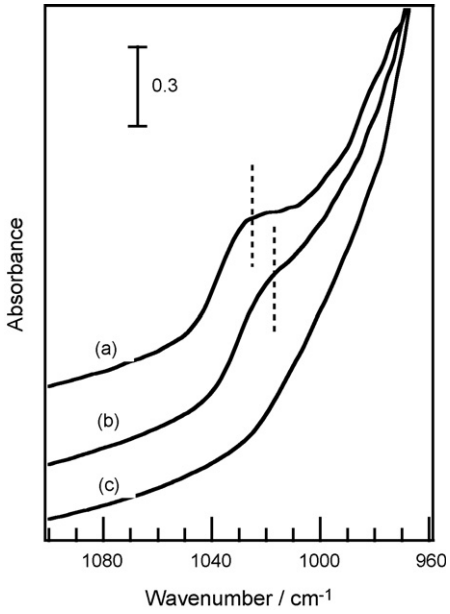

Fig. 7. FT–IR spectra of Rb-3.5VA catalysts at dehydrated state: (a) Rb/V = 0, (b) Rb/V = 0.5, and (c) Rb/V = 1.5.

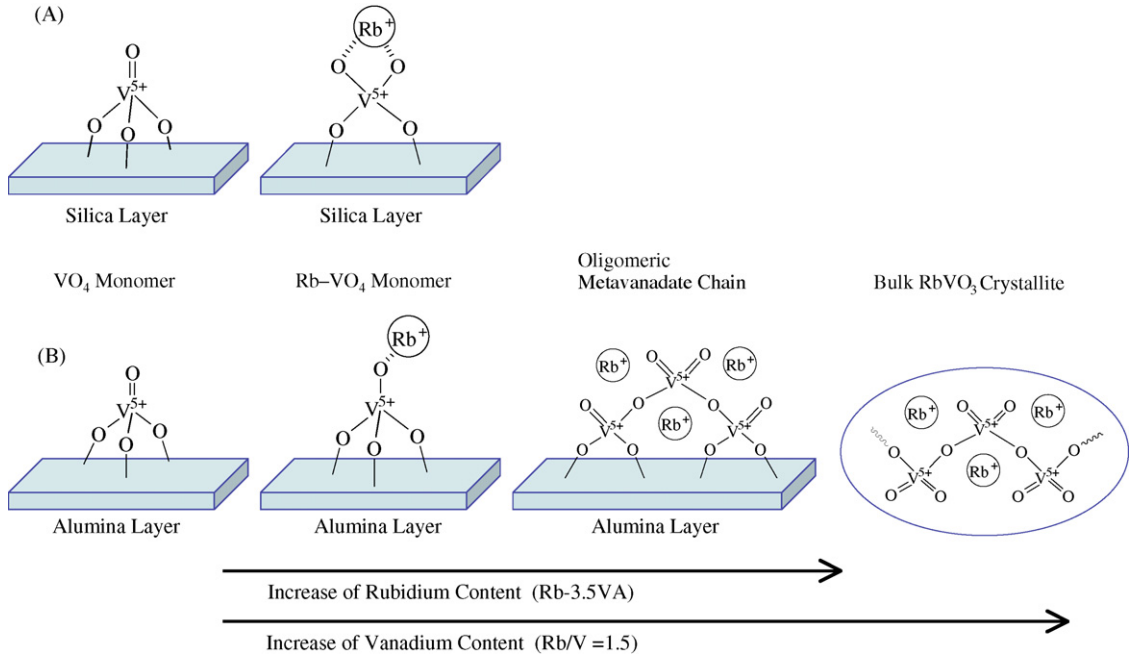

Fig. 8. Proposed molecular structure of surface vanadium oxide species in Rb-VS (A) and Rb-VA (B).

Parts B and C of Fig. 6 show k^3-weighted V-K edge EXAFS spectra and the Fourier transforms of dehydrated samples with 2.5 wt% of V_2O_5 loading. In contrast to XANES, there are differences between the absence and the presence of Rb ion in the EXAFS spectra. The EXAFS feature of 2.5VS was drastically changed by the Rb ion addition. In the case of 2.5VA, the features are slightly changed and the oscillation becomes clear. The local structure of vanadium atom can be visualized by the Fourier transforms of the EXAFS spectra to obtain radial structure function (RSF). All the RSF spectra show the peaks around 1–2 Å related to the scattering from the oxygen atoms in the first coordination sphere. The absence of the peaks at >2 Å indicates that the vanadium species are in a highly dispersed form. We carried out curve-fitting analysis of the Fourier-filtered EXAFS spectra (ΔR = 0.9–1.9). The results are summarized in Table 2. In the case of 2.5VS, there are two kinds of bond lengths, 1.62 and 1.81 Å. The shorter one has a double-bond character. The result of Rb-2.5VS shows the presence of two short bonds (1.65 Å) and two long bonds (1.87 Å). The bond length of the monomeric VO_4 species was drastically changed by Rb ion addition, even though the tetrahedral symmetry was not changed (Fig. 6A). The interaction with Rb ion occurs an elongation of the terminal V=O bond and a shortening the one of basal V–O bonds in 2.5VS. The structure of alkali-ion-modified vanadium oxide on silica has been proposed to a monomeric VO_4 tetrahedron with two shorter V–O bonds interacting a Rb ion as shown in Fig. 8 [8]. This structure is well consistent to the presence of two LMCT absorption peaks in Rb-2.5VS. In the case of 2.5VA, the curve-fitting analysis shows that there are two kinds of bond lengths, a shorter bond (V=O, 1.56 Å) and three longer bonds (V–O, 1.72 Å). The terminal V=O bond was elongated by addition of Rb ion. However, the three of the basal V–O bonds were hardly affected. The V–O bonds of VO_4 tetrahedron are almost equivalent in Rb-2.5VA.

Fig. 7 shows FT-IR spectra of Rb-3.5VA at dehydrated state. The non-modified 3.5VA shows a V=O stretching absorption centered at 1035 cm^{-1} assigned to the monomeric VO_4 species. An addition of Rb ion causes the band shift to higher wavenumber, indicating an elongation of V=O bond by an interaction with Rb ion. When the Rb/V ratio was 1.5, the band was disappeared in Rb-3.5VA. This indicates that the Rb ions strongly interacted to the terminal V=O bonds of the monomeric VO_4 species and weakened the double-bond character.

By means of multi-technical characterization, the local structure of the photocatalytic active site could be concluded to be Rb-ion-modified VO_4 monomers bound to alumina surface by three bonds as shown in Fig. 8B. It was confirmed that there are oligomeric metavanadate chains in the samples with high V_2O_5 loading and high alkali content. Since the propenal yield was monotonically increased with V_2O_5 loading until 3.5 wt% (Fig. 2) and with Rb/V molar ratio until 1.5 (Fig. 3), the metavanadate chains are not supposed to exhibit photocatalytic activity. In the case of Rb-VA with very high loading of V_2O_5, we observed the XRD patterns due to bulk $RbVO_3$ crystallite. The crystal sizes in Rb-10VA and Rb-20VA were determined to be 406 and 490 Å using Scherrer equation, respectively. The bulk $RbVO_3$ crystallite itself did not show photocatalytic activity (Table 1).

4. Conclusion

Similar to the result of alkali-ion-modified V_2O_5/SiO_2, an addition of alkali ion on V_2O_5/Al_2O_3 significantly enhanced the photocatalytic activity of the selective oxidation of propylene.

This suggests that the direct modification of the surface vanadium oxide species by an alkali ion is very powerful tool for tuning the physico-chemical properties. The Rb-ion-modified VO_4 monomers are determined to be the photocatalytic active sites for propenal production in the photocatalytic oxidation of propylene with molecular oxygen. The molecular structures of the surface vanadium oxide species are dependent both on the V_2O_5 loading and the alkali ion content in alkali-ion-doped V_2O_5/Al_2O_3. The metavanadate chains exhibit very low photocatalytic activity.

Acknowledgement

X-ray absorption experiments were performed at the Photon Factory with the approval of the High Energy Accelerator Research Organization (PF PAC Proposal No. 2003G077).

References

[1] J.C. Vedrine, J.M.M. Millet, J.C. Volta, Catal. Today 32 (1996) 115.
[2] A. Corma, H. Garcia, Chem. Rev. 102 (2002) 3837.
[3] T. Blasco, J.M.L. Nieto, Appl. Catal. A 157 (1997) 117.
[4] J.M.L. Nieto, P. Concepcion, A. Dejoz, F. Melo, H. Knozinger, M.I. Vazquez, Catal. Today 61 (2000) 361.
[5] G.G. Cortez, J.L.G. Fierro, M.A. Banares, Catal. Today 78 (2003) 219.
[6] X. Wang, I.E. Wachs, Catal. Today 96 (2004) 211.
[7] G. Deo, I.E. Wachs, J. Catal. 146 (1994) 335.
[8] S. Takenaka, T. Tanaka, T. Yamazaki, T. Funabiki, S. Yoshida, J. Phys. Chem. B 101 (1997) 9035.
[9] D.A. Bulushev, F. Rainone, L. Kiwi-Minsker, A. Renken, Langmuir 17 (2001) 5276.
[10] L. Lietti, P. Forzatti, G. Ramis, G. Busca, F. Bregani, Appl. Catal. B 3 (1993) 13.
[11] S. Takenaka, T. Kuriyama, T. Tanaka, T. Funabiki, S. Yoshida, J. Catal. 155 (1995) 196.
[12] A.M. Gritscov, V.A. Shvets, V.B. Kazansky, Chem. Phys. Lett. 35 (1975) 511.
[13] M. Krauss, Theochem 458 (1999) 73.
[14] A. Maldotti, A. Molinari, R. Amadelli, Chem. Rev. 102 (2002) 3811.
[15] K. Wada, H. Yamada, E. Watanabe, T. Mitsudo, J. Chem. Soc., Faraday Trans. 94 (1998) 1771.
[16] H.H. Lopez, A. Martinez, Catal. Lett. 83 (2002) 37.
[17] F. Amano, T. Tanaka, T. Funabiki, Langmuir 20 (2004) 4236.
[18] K. Tran, A.E. Stiegman, G.W. Scott, Inorg. Chim. Acta 243 (1996) 185.
[19] T. Tanaka, S. Takenaka, T. Funabiki, S. Yoshida, J. Chem. Soc., Faraday Trans. 92 (1996) 1975.
[20] T. Tanaka, T. Ito, S. Takenaka, T. Funabiki, S. Yoshida, Catal. Today 61 (2000) 109.
[21] F. Amano, T. Ito, S. Takenaka, T. Tanaka, J. Phys. Chem. B 109 (2005) 10973.
[22] F. Amano, T. Tanaka, Catal. Commun. 6 (2005) 269.
[23] K. Teramura, T. Tanaka, T. Yamamoto, T. Funabiki, J. Mol. Catal. A 165 (2001) 299.
[24] K. Teramura, T. Tanaka, M. Kani, T. Hosokawa, T. Funabiki, J. Mol. Catal. A 208 (2004) 299.
[25] K. Teramura, T. Tanaka, T. Hosokawa, T. Ohuchi, M. Kani, T. Funabiki, Catal. Today 96 (2004) 205.
[26] T. Tanaka, H. Yamashita, R. Tsuchitani, T. Funabiki, S. Yoshida, J. Chem. Soc., Faraday Trans. 84 (1988) 2987.
[27] J.M. Zhu, S.L.T. Andersson, J. Chem. Soc., Faraday Trans. 85 (1989) 3629.
[28] F. Marumo, M. Isobe, S. Iwai, Y. Kondo, Acta Cryst. B 30 (1974) 1628.
[29] M.A. Banares, I.E. Wachs, J. Raman Spectrosc. 33 (2002) 359.
[30] G.C. Bond, P. Konig, J. Catal. 77 (1982) 309.
[31] X.T. Gao, I.E. Wachs, J. Phys. Chem. B 104 (2000) 1261.
[32] J. Wong, F.W. Lytle, R.P. Messmer, D.H. Maylotte, Phys. Rev. B 30 (1984) 5596.